Res-UNet Based Optic Disk Segmentation in Retinal Image

Jia-Wen Lin[1,2], Xiang-Wen Liao[2], Lun Yu[1], Jeng-Shyang Pan[3*]

[1] College of Physics and Information Engineering, Fuzhou University, Fuzhou 350108, China

[2] College of Mathematics and Computer Science, Fuzhou University, Fuzhou 350108, China

[3] College of Computer Science and Engineering, Shandong University of Science and Technology, Qingdao 266590, China

Rose_wei7@126.com; liaoxw@fzu.edu.cn; cgifd@126.com; jspan@cc.kuas.edu.tw

Abstract. Automatic optic disk (OD) segmentation is an important tool for early detection of eye diseases. In this article, we proposed a Res-UNet network by applying residual learning module and other improvements in U-Net for optic disk segmentation in retinal image. Since training data available is insufficient, we enlarge the data set by generating data pieces. Res-UNet is then trained to classify each pixel of the input retinal image. Finally, the predicted probability map is further post-processed with morphological technique to get final OD segmentation result. Experiments on the public DRISHTI-GS data set including comparison with the best known methods show that the proposed model outperforms most existing methods on several metrics.

Keywords: morphology method, optic disk segmentation, residual learning, retinal image, U-Net

1 Introduction

Eye diseases, such as diabetic retinopathy and glaucoma, are the leading causes of blindness [1-2]. Without timely therapy, irreversible damage may lead to a loss of the visual field that could originate partial or total blindness. Hence, early detection and subsequent treatment is important to prevent visual damage. According to the study by the National Institutes of health and the National Eye Research Center, regular eye diseases screening should be received on time to ensure promote diagnosis [3-4].

Colorful fundus image is now widely used as a tool of collecting clinical information for assessment in screening. The optic disc (OD) is one of the main anatomical structures in retina [5]. As a retinal image shown in Fig. 1, in normal conditions, OD always appears as a bright yellowish disk and a relatively circular, and is the entry point of the major blood vessels [6].

Accurate OD segmentation takes the most valuable place in eye diseases screening and analysis of retinal image. The segmented OD provides an invaluable help for detecting other important structures of the retina and many lesions of the retina [4, 6]. For example, as the convergence of retinal vessels, OD can be used for vessel tracking. Automatic image registration and measurements for treatment evaluation are also benefit [4]. However, it is time-consuming for professionals to achieve OD segmentation. According to [7], full segmentation of OD cost per eye cost a skilled grader about 8 minutes. What's more, trained retinal image readers are always in limited worldwide and expensive [4].

Therefore, for more rapid and cost effective, automated retinal image analysis including automatic OD segmentation are essential in computer-aided diagnosis of retinal diseases. Automation would allow the primary care physicians to devote more time to real-time communication and education with patients [8].
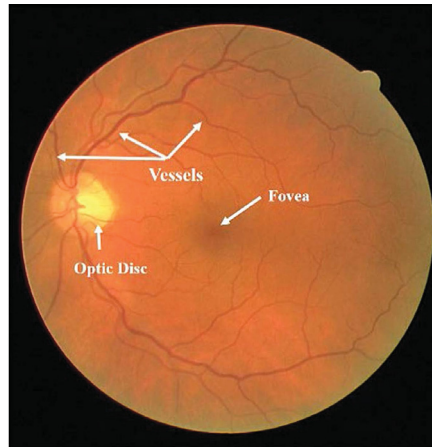
---

* Corresponding Author

Fig. 1. A colorful fundus image

1.1 Prior Related Work

Numbers of automated OD segmentation algorithms have been investigated in the past few decades. In most studies, the OD was identified with the features including shape, brightness and size. The state of art techniques are always categorized into 3 groups: template-based methods, morphology-based methods and deformable model-based methods.

Initial attempts have been made with template-based techniques. According to the common shape the OD, it is modeled as an elliptical or circular object, then a matching is performed. Pinz et al. [9] and Lalonde et al. [10] employed a Hough transform to detect the OD boundaries. An ellipse or a circle were applied by Wong et al. [11] and Morales et al. [12] to fit the boundary. However, some part of real OD may be missed since OD boundaries are not strictly circle or ellipse. Besides, these approaches may also fail to characterize shape due to the vessels appeared in and around the OD region and some pathological changes.

To overcome this limitation, morphological based techniques occurred. Both bright- ness and shape property of OD are used. Morphological operators is employed to suppress the vessel as a preprocessing step, so that an isolated circular bright region can be detected [13-14]. These methods suffer due to bright lesions which take the similar appearance with OD. Sometimes, the area of optic disk may be mistakenly find while other matter is of higher brightness.

Deformable model-based techniques were proposed to achieve more accurate OD segmentation [6]. Lowell et al. [15] segmented OD boundary with a local deformation model and a preprocessing step by constraining the result to an elliptical object. A modified active shape model is proposed by Li et al. [16] to get a smoother boundary, while PCA is first introduced to build the shape model based on the training images. Esmaeili et al. [17] used a vibrational level set model to obtain a more accurate OD boundary. Joshi et al. [18] present a region-based active contour model to get the OD boundary, enhancing the scope of the C-V model by including image information at support domain around each point of interest. Literature [19] proposed an active-disc-based formalism for OD segmentation. By using gradient descent technique enhancement is achieved, and the matched filtering technique helps to decide the initialization of the active disc. In 2018, Cao et.al [20] generated saliency map by using intensity, color and spatial distribution of the disc, and then segment OD with the adaptive threshold. A rotary scanning method is finally devised to achieve continuous contour of optic disk boundary. Although deformable model-based methods achieve satisfied results, they may fail because of the interferences around OD region. These methods always need much time and their performances always depend upon contour initialization.

Machine learning approaches were introduced to gain a more powerful feature classification tool. After removing vessel, Bock et al. [21] got different generic features extract based on PCA method, and then these features were combined into a probabilistic two-stage classification scheme. Carefully hand crafted features ensure the success of machine learning methods to detect OD. Cheng et al. [22] present a superpixel based classification method for OD segmentation. Mahapatra et al. [23] introduced random forest classifier to construct special optic disc segmentation model while Sedai et al. [24] presented a regression based OD segmentation method. However, such algorithms with hand crafted features do not generalize well when referring to different datasets.

Convolution Neural Network (CNN) and deep learning algorithms have become popular in image and video processing as discriminative features can be available [25]. Many feasible approaches based on deep learning are applied to automatic retinal image analyzing [26]. To handle OD segmentation problem, Maninis et al. [26] employ fully-convolutional neural network based on VGG-16-net and transfer learning technique. Zilly et al. [27] proposed 2-layer multi-scale convolutional neural network (CNN) for segmentation. While training, an entropy sampling technique is used to reduce computational complexity. In [28], they present an improvement in the training procedure. However, method from [26] takes a long time to train the model. Models from of [27-28] are so complicated that the reported results are difficult to reproduce. Although prepared for execution on CPU, they will have large prediction time. In 2017, Sevastopolsky [29] firstly introduced U-Net convolutional neural network to handle the OD boundary detection with simple framework. A lowest prediction time, which has outperformed all the state of the art, was reached. However, the overlap between the automatic segmented result and the manual ground truth is not satisfied.

Above all, for both high accuracy and low computational time, OD segmentation is still challenging. Methods based on deep learning techniques are worth exploring.

1.2 Our Work

In this paper, we propose a more efficient method to detect the OD. The ResNet combined with U-Net composes a pixel-wise OD segmentation model. Experiments demonstrate the effectiveness of our approach. Our method differs from the existing researches in the following aspects:

- In order to improve the learning ability and training efficiency of the network, we proposes Res-UNet by introducing the residual learning module of ResNet to modify the U-Net architecture. So there is no need to design hand crafted features since the optimal representational features through the filters are learned through the network.
- Considering the insufficient samples, we generate data pieces by rotating and intercepting images to extend the training set. It is a key step for training the network.
- For each retinal image, a segmentation map is obtained through the trained classifier. Since some blobs around the retinal image edge or lesions are bright, the OD may be confuse with them. Therefore, Morphological processing is finally con- duct to the segmentation map, eliminating the disturbance pixels for an excellent segmentation.

The rest of our paper is organized as follows. In Section 2, the framework of our proposed method is described briefly, and the details of each part of our model, including pre-processing, network architecture, training and segmentation procedure, and post- processing are also given. Experiments and results are shown in Section 3. Finally, we end with a conclusion and discussion in Section 4.

2 Proposed Method

Fig. 2 shows the framework of our proposed OD segmentation model. The method can divides into the training stage and segmentation stage, composing of several modules.

- Preprocessing module conduct a series of transformations to the original input fundus images.
- Data augmentation module helps to extend the data set for training efficiently.
- Res-UNet plays a core role in our method. For a retinal image as input, the output of the trained network can be seen as the initial segmentation result.
- Post−processing by morphological method achieves the final OD segmentation map.

2.1 Pre-processing

Before being sent to Res-UNet, there are several preprocessing steps should be done to the original colorful retinal image. According to Eqn. (1) and Eqn. (2), normalization is firstly applied to the gray image of a retinal image.
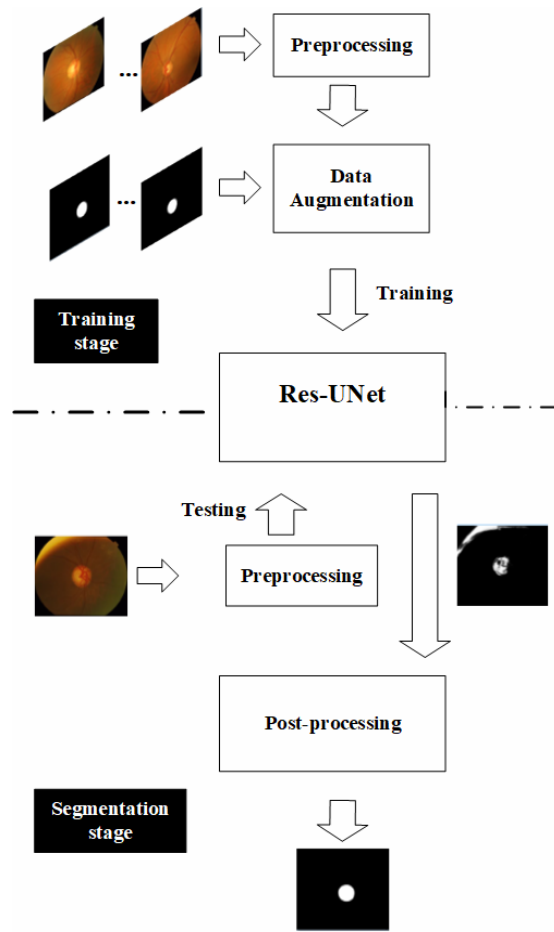
$$f = \left(I - I_{mean} \right) / I_{std} \tag{1}$$

Fig. 2. Framework of the proposed OD segmentation model using Res-UNet

$$I_{normalized} = \frac{f - f_{min}}{f_{max} - f_{min}} \tag{2}$$

where I_{mean} is the average of I, I_{std} is the standard deviation of the image and $I_{normalized}$ means the normalized image.

Secondly, contrast limited adaptive histogram equalization (CLAHE) method is employed for image enhancement. In the end, the gamma adjustment is made by Eqn. (3).

$$I_{processed} = \left(\frac{I_{normalized}}{255}\right)^{-\alpha} * 255 \tag{3}$$

Fig. 3 shows the preprocessing of a retinal image. The improved image is required in the data augmentation or segmentation stage as input data.
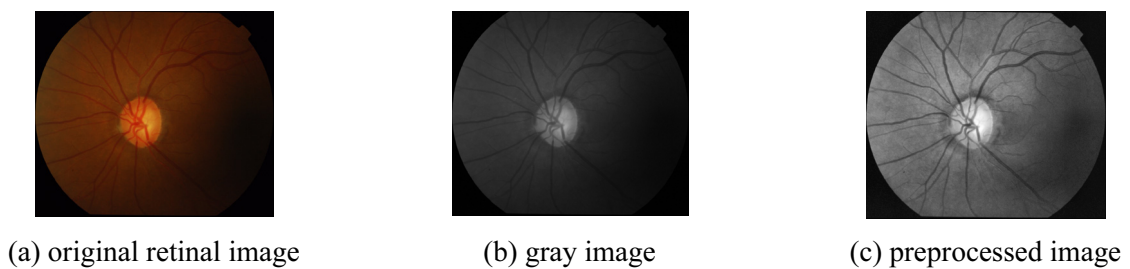

| (a) original retinal image | (b) gray image | (c) preprocessed image |

Fig. 3. Illustration of the results of pre-processing

2.2 Data Argumentation

As for OD segmentation, there is insufficient available training data. Data augmentation is essential to overcome the shortage of training set. In this work, the overlapping sampling strategy is adopt to increase the robustness of the model.

First of all, we rotate the images in training set by $0°, 90°, 180°$ and $270°$. Thus, the new set is of 4 times number of pictures. Then, the image is sampled by sliding a 64x64 window with the stride of 8 pixels. Pieces will be filled in black automatically when its size does not match the window. Both fundus images and the corresponding masks have been augmented via elastic deformations to the available images. Although the pieces may locate out of the region of interest partially or entirely, they do not affect the training process. Samples of a retinal image and its mask are shown in Fig. 4.Each small square in the figure corresponds to an image piece.
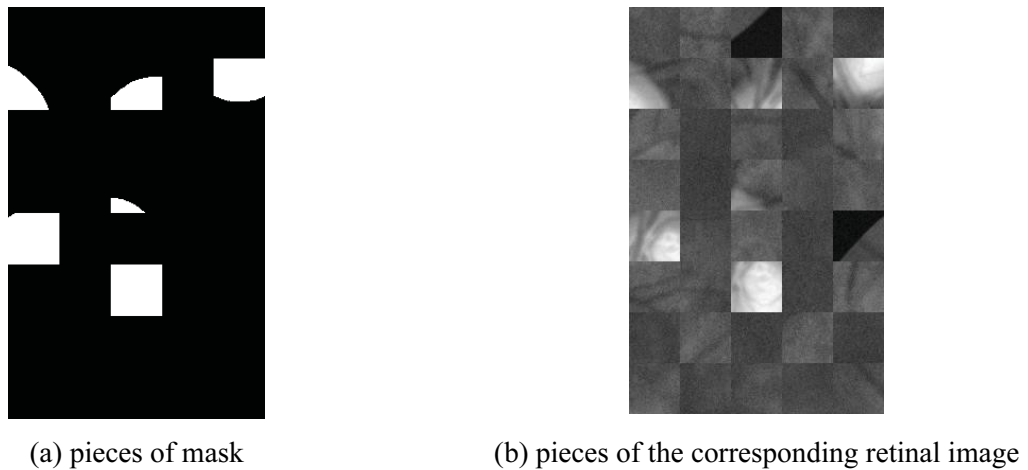

(a) pieces of mask   (b) pieces of the corresponding retinal image

Fig. 4. The sample of Pieces

2.3 Res-UNet

The U-Net network [30] proposed in 2015 is now widely used in medical image segmentation. It is suitable for data sets with only a few labels. It combines low-level feature vectors with high-level feature vectors through jump connection to produce accurate horizontal location of pixels. However, the original architecture lacks of higher learning capacity. Deep residual network (Res-Net) [31] can avoid gradient vanishing or exploding during training, and has been successfully applied in medical image analysis. Here, we present a new network called Res-UNet by integrating residual block of ResNet into the U-Net. Through Res-UNet, all the pixels of a retinal image are supposed to assign to two classes: optic disc and background.

Architecture. The architecture of the proposed network is presented in Fig. 5. The Res-UNet is based on the typical U-Net architecture, including encoder procedure in the left and decoder in the right.
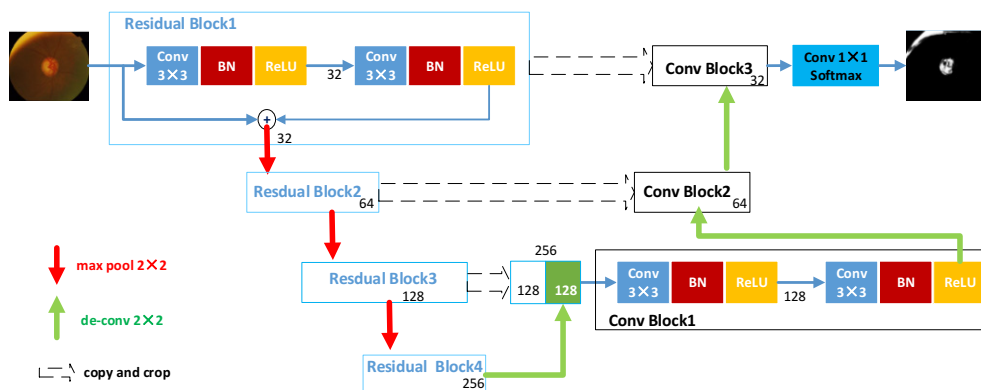

Fig. 5. Architecture of Res-UNet

In the left side, three residual blocks are adopt as the main body of our model. Each block consists of multiple 3x3convolutional layers, rectified linear units (ReLU) [32] and batch normalization (BN) layers [33]. Different from original U-Net, a shortcut connection is added, which performs the identity mapping of the input and element-wise addition to the output of the block. Repeated pooling operation is implemented for down sampling.

In the right side, the decoder procedure includes three convolutional blocks and repeated application of up-sampling for increasing the image resolution. For each convolutional block, it takes two outputs as its input: 1) the output of the last block in the encoder; 2) the correspondingly cropped feature map from the contracting path. Due to the loss of border pixels during every convolution, the cropping with the high-resolution features of the left structure help to get more accurate features. The information of the front layer and the back layer are crossed, so positioning will be better.

Loss Function. In this work, two loss functions are defined. Firstly, since OD segmentation can be regarded as the problem of binary classification of each pixel in fundus image, the cross-entropy function is used. The cross entropy can optimize the classification based on Eqn. (4).

$$H = -\frac{1}{n}\sum(y_i \log \hat{y}_i + (1 - y_i)\log(1 - \hat{y}_i)) \tag{4}$$

where y_i is the binary label of pixel i while $\hat{y}_i$ denotes the prediction probability of the pixel.

The Jaccard Similarity Coefficient (J) can be seen as a measure of similarity between finite sets. For a better OD segmentation result, J is introduced as another loss function to minimize the error between the probability map and the ground truth. Here, the function can be expressed as Eqn. (5).

$$J = \frac{1}{n}\sum_{i=1}^{n}(\frac{y_i\hat{y}_i}{y_i + \hat{y}_i - y_i\hat{y}_i}) \tag{5}$$

The two loss functions above are combined to get the final loss function as (6). The lower the value of L, the better the prediction. Afterwards, the corresponding weights are used to make the prediction.

$$L = H - \log J \tag{6}$$

2.4 Prediction of the Network

For prediction, both input and output of the network are pieces. Following preprocessing, original image is cut into pieces of size 64×64 every 8 pixels, and then is sent to the model. The output pieces can be assembled according to the size of the piece and the stride. The black part caused by the size mismatch in the data argumentation process is removed.

As mention above, the probability distribution over two classes could be given through the network. The resulting probability map of OD is displayed in Fig. 6(a).
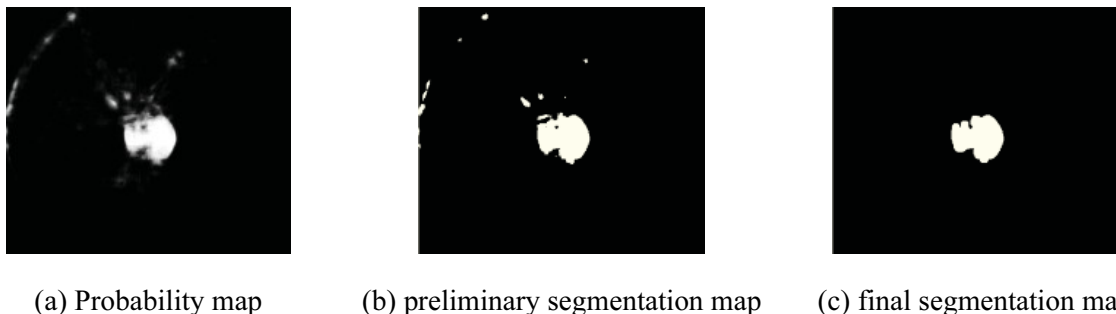

(a) Probability map   (b) preliminary segmentation map   (c) final segmentation map

Fig.6. OD segmentation result

2.5 Post-Processing

As Fig. 6 shown, it is obvious that some non-OD pixels are included in the predict OD segmentation map. The confusions appear because that some lesions, noise and blobs close to the image edge share some

characteristics with OD. They may have similar texture or color. However, we can distinguish the true OD from other region by their shape.

To make prediction more accurate, the OSTU method is firstly applied to the probability map to get the preliminary binary segmentation map. Then a morphological opening with a disk element is operated to the binary predicted map for eliminating the disturbance pixels. The radius of disk element is determined experimentally. It is found that the radius of disk element for effective segmentation could be set as half of the actual size of OD radius. With post-processing, the interference can be removed to obtain the final OD region. Fig. 6(b) and Fig. 6(c) presents the post-processing to get the final segmentation region of OD.

3 Experiments

3.1 Dataset and Experimental Environment

The evaluation of the proposed model has been conducted on the public database DRISHTI-GS dataset [34]. The database contains a total of 100 patient retinal images using 30 degree FOV at a resolution of 2896 x 1944. The entire dataset is divided into a training set called DGS-training group and a testing set called DGS-testing group. Each subset consists of 50 images. The DGS-training group provides every image a mask determined by 4 experts. During data argumentation, every image can generate 83780 image pieces by overlapping sampling.

The presented algorithm were implemented on an intele31231v3 CPU running Windows 10, with Keras framework and Python for training of U-Net. All estimates of computational time are given with NVDIA GeForce GTX 1080 graphics and 32 G memory.

3.2 Evaluation Criteria

Quantitative evaluation of each segmentation by our method is in terms of Specificity (*Spe*), Recall (*R*), Precision (*P*) and F-score (*F*). These performance metrics are defined as below:

$$Spe = \frac{TN}{TN + FP} \tag{7}$$

$$R = \frac{TP}{TP + FN} \tag{8}$$

$$P = \frac{TP}{TP + FP} \tag{9}$$

$$F = \frac{2P \times R}{P + R} \tag{10}$$

where *TP* and *TN* show the correct OD pixels and background pixels which are consistent with the ophthalmologists judgments. And *FP* and *FN* count the wrong OD pixels and the background which is inconsistent with the manual mask. F-score is computed as the harmonic mean of precision and recall, and value range in [0, 1]. Higher value of the metrics mentioned above indicate the better performance.

The overlap measure (*S*) is calculated as (11) defined:

$$S = \frac{Area(M \cap A)}{Area(M \cup A)} \tag{11}$$

where *M* and *A* correspond to the manually obtained OD region and the region determined by our method respectively.

Additionally, computation time *T* indicates the time required for the segmentation stage measured in seconds.

3.3 Results and Analysis

Firstly, the proposed method were applied to the DGS-training group. Here, we took a 5 fold cross validation scheme. The DGS-training group is divided into 5 folds, in which there are 10 images. Each time one fold was used for training stage while the remaining four folds were involved in the segmentation stage. The average segmentation performance across all folds are computed.

Table 1 illustrates the overall performance by proposed method on the DGS-training group. The average F-score of our approach reaches 99.4% with an average overlap of 90.6% respectively. The ROC curve are draw in Fig. 7 to quantify to the performance of our model. The false positive rate is on the x-axis, whereas true positive rate is on the y-axis. The area under the curve (AUC) of the model is 0.998, which is very close to 1.

Table 1. Average performance of proposed method on DGS-training group

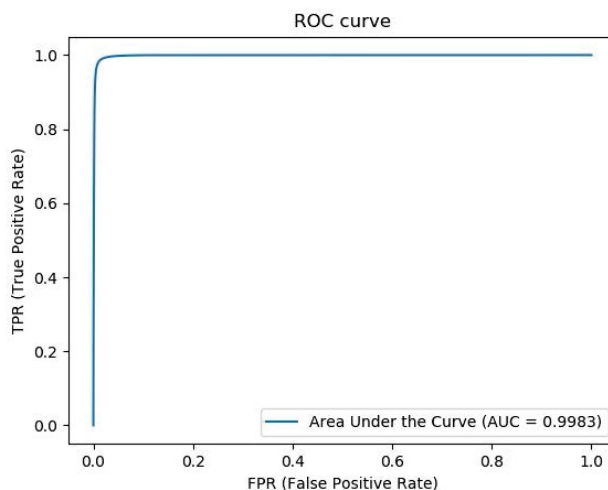|	*Spe*	*R*	*P*	*F*	*S*
Average value	99.6%	92.8%	89.1%	99.4%	90.6%

Fig. 7. The ROC curve of proposed model

The results of OD segmentation by different methods reviewed in literature on the same dataset are summarized in Table 2. We compare their performance in terms of F-score F, overlap S and computational time T, and also highlight the best performance. The comparative results suggest that our method performs better than most previous methods, and demonstrate quality competitive with other approaches in a majority of metrics. Especially, the proposed model outperforms all the competing algorithms list in Table 2 with the highest F-score. Overlap of proposed model compares well with the one presented in [28], which are based on the standard CNN architectures. However, the presented model achieve a higher F-score value with less computational time. This clearly indicates that Res-UNet architecture may be more effective for OD segmentation. Our method is more time consuming than [29] due to data argumentation and the post-processing, which are benefit for more accurate OD region.

Table 2. OD segmentation results on DGS-training group using different methods

Paper	Year	Method	*S* (%)	*F* (%)	*T* (s)
Joshi et al. [18]	2011	Active contours model	85	90.8	-
Cheng et al. [22]	2013	Superpixel	87.3	93.2	8
Mahapatra et al. [23]	2015	Random forest	89.5	95.9	7
Zilly et al. [27]	2015	CNN	89.5	94.7	-
Sedai et al. [24]	2016	Shape regression	–	95	–
Zilly et al. [28]	2017	Entropy sampling and CNN	**91.4**	97.3	5.3
Sevastopolsky [29]	2017	U-Net	75	-	**0.06**
Cao et al. [20]	2018	Visual saliency and rotary scanning	88.5	93.4	4
Proposed method	2019	Res-UNet	90.6	**99.4**	1.7

The best and worst segmented result are shown in Fig. 8. In the best case shown in the first row, a nearly perfect OD region is available. In the worst case, part of the OD is missing. The difference between the best and worst results is possibly due to the nerve fiber layer around OD. Sometimes, the poor quality of retinal image such as low contrast or the uneven brightness, also lead to the unsatisfactory segmentation results.
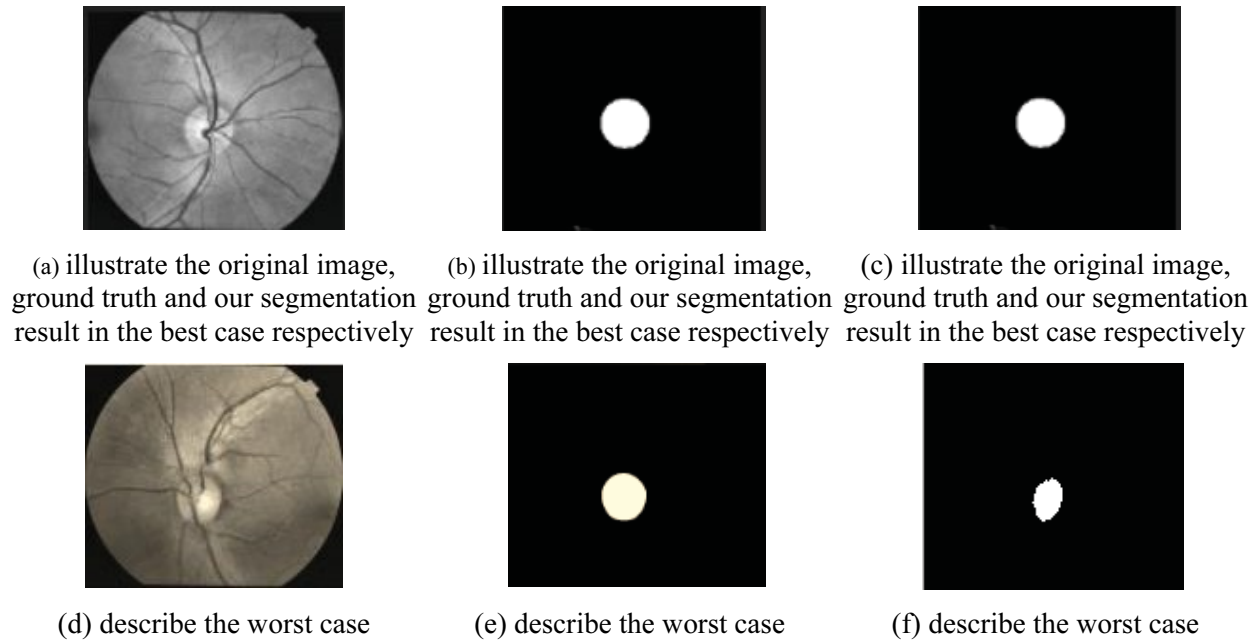

(a) illustrate the original image, ground truth and our segmentation result in the best case respectively

(b) illustrate the original image, ground truth and our segmentation result in the best case respectively

(c) illustrate the original image, ground truth and our segmentation result in the best case respectively

(d) describe the worst case

(e) describe the worst case

(f) describe the worst case

Fig. 8. Best/worst case of OD segmentation

To verify our approach further, the whole DGS-testing group was used for testing after the model had been trained based on the entire DGS-training group. Because there are no manual ground truth or other public mask, it is hard to make quantitative analysis of presented method. Several examples of OD segmentation on the DGS-testing group are displayed in Fig. 9. From overall results, proposed Res-UNet based model with morphological technique serve the task of OD segmentation effectively.
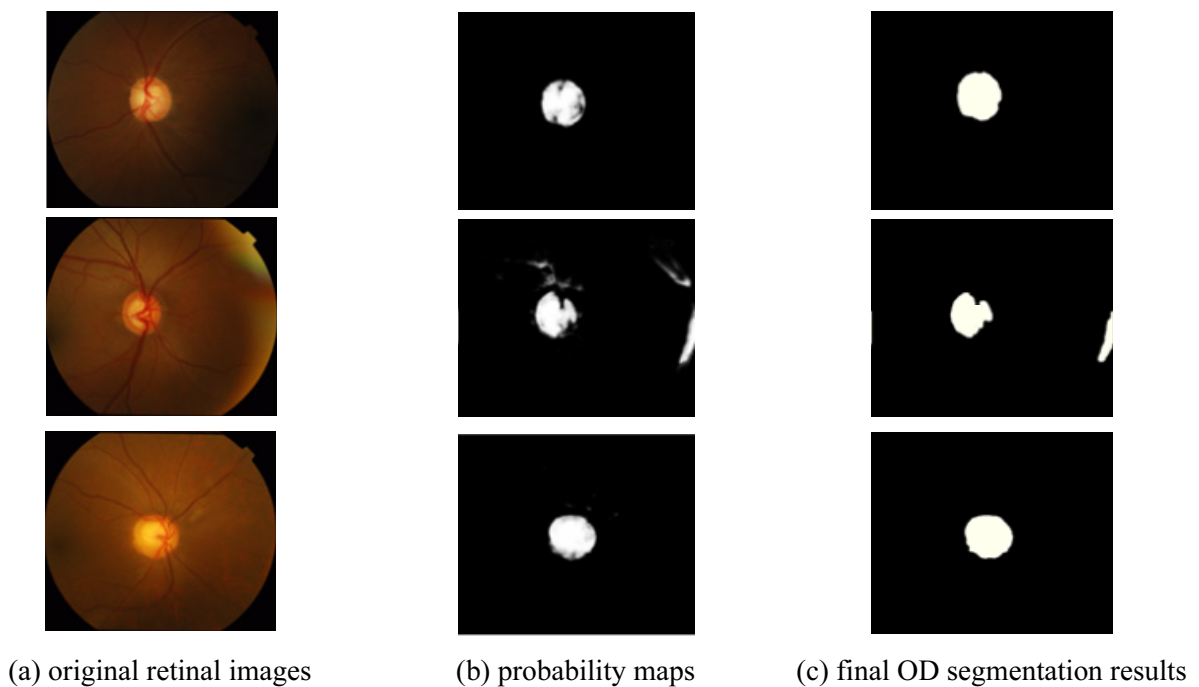

(a) original retinal images

(b) probability maps

(c) final OD segmentation results

Fig. 9. Examples of OD segmentation on the DGS-testing group

4   Conclusion and Discussion

In this paper, by combining the popular ResNet and U-Net architectures, a modified network called Res-UNet is developed for automatic optic disc segmentation in retinal images. By generating data pieces, small datasets can be used for network training. And post-processing with morphology methods make accurate OD region available. Experiments show that proposed model achieves high quality of segmentation on the DRISHTI- GS dataset and outperform most existing algorithms with high accuracy and low computational time.

Although the proposed method perform well, there are still some limitations to be cover. Firstly, the probability map as output of Res-UNet is sometimes prone to be discontinuous due to bloods, lesions and nerve fiber layer around OD, whereas some incorrect pixels may be included. The proposed post-processing may reduce the real OD region when removing interferences. In the future, techniques such as graph cut algorithm may be inspired in post-processing for a more reliable segmentation result, including filling empties in OD region and smoothing edges. Then, the Res-UNet was trained with only 50 images. Not all the variability of retinal images can be represented in the data set. Thus, we should apply our model to other larger database. Improvements of the network architecture and data argumentation are still challenges for more reliable and robust framework. Besides, the proposed model can be extended to segment the optic cup in the OD region in the future.

Acknowledgements

References

[1]   A. Almazroa, R. Burman, K. Raahemifar, V. Lakshminarayanan, Optic disc and optic cup segmentation methodologies for glaucoma image detection: a survey, Journal of Ophthalmology 7(2015) 1-28.

[2]   N. Cho, J. Shaw, S. Karuranga, Y. Huang, J. da Rocha Fernandes, A. Ohlrogge, B. Malanda, IDF diabetes atlas: Global estimates of diabetes prevalence for 2017 and projections for 2045, Diabetes research and clinical practice 138(2018) 271-281.

[3]   G.G. Yen, W.-F. Leong, A sorting system for hierarchical grading of diabetic fundus images: A preliminary study, IEEE Transactions on Information Technology in Biomedicine 12(1)(2008) 118-130.

[4]   D.A. Sim, P.A. Keane, A. Tufail, C.A. Egan, L.P. Aiello, P.S. Silva, Automated retinal image analysis for diabetic retinopathy in telemedicine, Current Diabetes Reports 15(3)(2015) 1-9.

[5]   S.D. Bharkad, Automatic segmentation of optic disk in retinal images using dwt, in: Proc. the 13th IEEE International Conference on Advanced Computing, 2016.

[6]   H. Yu, E.S. Barriga, C. Agurto, S. Echegaray, M.S. Pattichis, W. Bauman, P. Soliz, Fast localization and segmentation of optic disk in retinal images using directional matched filtering and level sets, IEEE Transactions on information technology in biomedicine 16(4)(2012) 644-657.

[7]   G. Lim, Y. Cheng, W. Hsu, M.L. Lee, Integrated optic disc and cup segmentation with deep learning, in: Proc. the 27th IEEE International Conference on Tools with Artificial Intelligence, 2015.

[8]   P.S. Silva, J.D. Cavallerano, L.M. Aiello, L.P. Aiello, Telemedicine and diabetic retinopathy: moving beyond retinal screening, Archives of ophthalmology 129(2)(2011) 236-242.

[9]   A. Pinz, S. Bernogger, P. Datlinger, A. Kruger, Mapping the human retina, IEEE Transactions on Medical Imaging 17(4)(1998) 606-619.

[10] M. Lalonde, M. Beaulieu, L. Gagnon, Fast and robust optic disc detection using pyramidal decomposition and hausdorff-based template matching, IEEE transactions on medical imaging 20(11)(2001) 1193-1200.

[11] D. Wong, J. Liu, J. Lim, X. Jia, F. Yin, H. Li, T. Wong, Level-set based automatic cup-to-disc ratio determination using retinal fundus images in argali, in: Proc. the 30th Annual International Conference of the IEEE Engineering in Medicine and Biology, 2008.

[12] S. Morales, V. Naranjo, J. Angulo, M. Alcan~iz, Automatic detection of optic disc based on PCA and mathematical morphology, IEEE Transactions on Medical Imaging 32(4)(2013) 786-796.

[13] R. Abdel-Ghafar, T. Morris, Progress towards automated detection and characterization of the optic disc in glaucoma and diabetic retinopathy, Medical Informatics and the Internet in Medicine 32(1)(2007) 19-25.

[14] D. Welfer, J. Scharcanski, D.R. Marinho, A morphologic two-stage approach for automated optic disk detection in color eye fundus images, Pattern Recognition Letters 34(5)(2013) 476-485.

[15] J. Lowell, A. Hunter, D. Steel, A. Basu, R. Ryder, E. Fletcher, L. Kennedy, Optic nerve head segmentation, IEEE Transactions on Medical Imaging 23(2)(2004) 256-264. DOI:10.1109/TMI.2003.823261

[16] H. Li, O. Chutatape, Boundary detection of optic disk by a modified ASM method, Pattern Recognition 36(9)(2003) 2093-2104.

[17] M. Esmaeili, H. Rabbani, A.M. Dehnavi, Automatic optic disk boundary extraction by the use of curvelet transform and deformable variational level set model, Pattern Recognition 45(7)(2012) 2832-2842.

[18] G.D. Joshi, J. Sivaswamy, S. Krishnadas, Optic disk and cup segmentation from monocular color retinal images for glaucoma assessment, IEEE transactions on medical imaging 30(6)(2011) 1192-1205.

[19] J.H. Kumar, A.K. Pediredla, C.S. Seelamantula, Active discs for automated optic disc segmentation, in: Proc. 4th IEEE Global Conference on Signal and Information Processing, 2015.

[20] X. Cao, L. Xue, J. Lin, L. Yu, A novel method of optic disk segmentation based on visual saliency and rotary scanning, Journal of Biomedical Engineering 35(2)(2018) 229-236.

[21] R. Bock, J. Meier, L.G. Nyúl, J. Hornegger, G. Michelson, Glaucoma risk index: automated glaucoma detection from color fundus images, Medical Image Analysis 14(3)(2010) 471-481.

[22] J. Cheng, J. Liu, Y. Xu, F. Yin, D.W.K. Wong, N.-M. Tan, D. Tao, C.-Y. Cheng, T. Aung, T.Y. Wong, Superpixel classification based optic disc and optic cup segmentation for glaucoma screening, IEEE Transactions on Medical Imaging 32(6)(2013) 1019-1032.

[23] D. Mahapatra, J.M. Buhmann, A field of experts model for optic cup and disc segmentation from retinal fundus images, in: Proc. the 12th IEEE International Symposium on Biomedical Imaging (ISBI), 2015.

[24] S. Sedai, P.K. Roy, D. Mahapatra, R. Garnavi, Segmentation of optic disc and optic cup in retinal fundus images using shape regression, in: Proc. the 38th Annual International Conference of the IEEE Engineering in Medicine and Biology Society (EMBC), 2016.

[25] K. Simonyan, A. Zisserman, Very deep convolutional networks for large-scale image recognition, in: Proc. the International Conference on Learning Representations (LCLR), 2015.

[26] KK. Maninis, J. Pont-Tuset, P. Arbelaéz, L. Van Gool, Deep retinal image understanding, in: Proc. the 19th International Conference on Medical Image Computing and Computer-assisted Intervention (MICCAI), 2016.

[27] J. Zilly, J. Buhmann, D. Mahapatra, Boosting convolutional filters with entropy sampling for optic cup and disc image segmentation from fundus images, in: Proc. the 6th International Workshop on Machine Learning in Medical Imaging, 2015.

[28] J. Zilly, J.M. Buhmann, D. Mahapatra, Glaucoma detection using entropy sampling and ensemble learning for automatic optic cup and disc segmentation, Computerized Medical Imaging and Graphics 55(2017) 28-41.

[29] A. Sevastopolsky, Optic disc and cup segmentation methods for glaucoma detection with modification of u-net convolutional neural network, Pattern Recognition and Image Analysis 27(3)(2017) 618-624.

[30] O. Ronneberger, P. Fischer, T. Brox, U-net: Convolutional networks for biomedical image segmentation, in: Proc. the 18th International Conference on Medical Image Computing and Computer-assisted Intervention (MICCAI), 2015.

[31] K. He, X. Zhang, S. Ren, J. Sun, Deep residual learning for image recognition, in: Proc. the IEEE Conference on Computer Vision and Pattern Recognition (CVPR), 2016.

[32] K. Hara, D. Saito, H. Shouno, Analysis of function of rectified linear unit used in deep learning, in: Proc. the International Joint Conference on Neural Networks, 2015.

[33] S. Ioffe, C. Szegedy, Batch normalization: Accelerating deep network training by reducing internal covariate shift, in: Proc. the 32nd International Conference on Machine Learning (ICML), 2015.

[34] J. Sivaswamy, S. Krishnadas, G.D. Joshi, M. Jain, A.U.S. Tabish, Drishti-GS: Retinal image dataset for optic nerve head (ONH) segmentation, in: Proc. the 11th International Symposium on Biomedical Imaging (ISBI), 2014.